



## Review article

## A systematic review on the current status of PSMA-targeted imaging and radioligand therapy

Giuseppe Capasso<sup>a</sup>, Azzurra Stefanucci<sup>b,\*</sup>, Anna Tolomeo<sup>a</sup><sup>a</sup> ITEL TELECOMUNICAZIONI S.r.l – Radiopharmaceutical Division, Italy<sup>b</sup> Department of Pharmacy, Università degli Studi “G. d’Annunzio” Chieti, Pescara, Italy

## ARTICLE INFO

## Keywords:

Prostate cancer imaging  
 Prostate specific membrane antigen  
 Positron emission tomography  
 Radioligand Therapy  
 Theranostics

## ABSTRACT

Prostate specific membrane antigen (PSMA) has been the subject of several studies in recent decades as a promising molecular target for prostate cancer (PCa), in fact it is considered an excellent molecular target for both PCa imaging (both for staging and follow-up), by means of PET/CT and for radioligand therapy. Its interesting molecular features have enabled the development of a new diagnostic and therapeutic approach for PCa, called “theranostics.” Considering the abundance of PSMA-based probes that have appeared so far in the literature, the present work focuses the attention on radiopharmaceuticals with increasing clinical application, highlighting advantages and disadvantages in terms of different metabolism and excretion processes, pharmacokinetic, binding affinity and variable internalization rate, tumor-to-background ratio, residence times and toxicity profile.

## 1. Introduction: PSMA as an excellent target for prostate cancer imaging

Within the large overview of the most prevalent diseases of the last millennium, prostate cancer (PCa) is the second diagnosed cancer and the fifth leading cause of cancer death among men worldwide [1]. Prostate-specific antigen (PSA) is currently the most commonly used biomarker for PCa screening, as well as a reliable marker for disease recurrence after initial treatment [2].

Prostate-specific membrane antigen (PSMA) is up-regulated in poorly differentiated, metastatic and hormone-refractory PCa (CRPC), although it may also be low-expressed in other healthy organs, such as salivary and lacrimal glands, proximal small intestine, kidney, brain, liver and spleen thus it could be involved in other tumour pathologies or benign processes. For these reasons, PSMA is considered an excellent molecular target for PCa imaging, both for staging and follow-up purposes [3], by positron emission tomography/computed tomography (PET/CT), as well as for radioligand therapy [1].

Radiopharmaceuticals targeting PSMA, due to its overexpression on prostate cancer cells based on the stage and degree of tumour progression (Gleason Score) in androgen-independent, advanced and metastatic disease, have been developed and transferred to the clinic.

Prostate-specific membrane antigen (PSMA) is a transmembrane

glycoprotein (also called glutamate carboxypeptidase II (GCPII), N-acetyl-L-aspartyl-L-glutamate peptidase I or NAAG peptidase), with glutamate carboxy-peptidase activity, able to regulate intestinal folate absorption and also catalysing the hydrolysis of N-acetyl-L-aspartyl-L-glutamate (NAAG) into N-acetyl-L-aspartate and L-glutamate, which is an important excitatory neurotransmitter of the central nervous system (CNS) [4].

Recent crystallographic studies of complexes between GCPII and low-molecular-weight ligands [5] have shown the high affinity of the receptor substrate PSMA for negatively charged amino acids such as aspartate and glutamate at the level of the S1' pocket, which acts as a pharmacophore (Fig. 1) and it is composed by Arg534, Arg536 and Arg463, so-called “arginine patch” [4].

The S1 pocket of GCPII, on the other hand, is flexible and better suited for structural modifications of GCPII inhibitors. In fact, residue Arg536 can adopt two distinct conformations, referred to as the “stacking” conformation and the “binding” conformation. The “stacking” conformation of Arg536 renders this residue unavailable for substrate binding, forcing its guanidinium group to be embedded between Arg534 and Arg463. This conformation is further stabilized by ionic interaction with the carboxylate of Asp465 and hydrogen bonding with the carbonyl oxygen of Arg463 [6].

The transition between these two conformations of Arg 536 is associated with the side-chain shift of Arg463 among the “up” and “down”

\* Corresponding author.

E-mail addresses: [g.capasso@itelte.it](mailto:g.capasso@itelte.it) (G. Capasso), [a.stefanucci@unich.it](mailto:a.stefanucci@unich.it) (A. Stefanucci), [a.tolomeo@itelte.it](mailto:a.tolomeo@itelte.it) (A. Tolomeo).<https://doi.org/10.1016/j.ejmech.2023.115966>

Received 24 July 2023; Received in revised form 13 November 2023; Accepted 14 November 2023

Available online 17 November 2023

0223-5234/© 2023 The Authors.

Published by Elsevier Masson SAS. This is an open access article under the CC BY license (<http://creativecommons.org/licenses/by/4.0/>).

### Abbreviations

PSMA	Prostate specific membrane antigen	acid	
Pca	Prostate Cancer	NOTA	1,4,7-triazacyclododecane-1,4,7-triacetic acid
PET/CT	Positron emission tomography/computerised tomography	HBED-CC	N,N'-bis-[2-hydroxy-5-(carboxyethyl)benzyl] ethylenediamine-N,N'-diacetic acid
PET/MRI	Positron Emission Tomography/Magnetic Resonance Imaging	RLT	Radioligand therapy
PSA	Prostate-specific antigen	LN	Lymph nodes
mCRPC	Metastatic Castration-Resistant Prostate Cancer	MeCN	Acetonitrile
GCPII	Glutamate carboxypeptidase II	BuOH	Butanol
NAAG	N-acetyl-L-aspartyl-L-glutamate	FDA	U.S. Food and Drug Administration
CNS	Central nervous system	EMA	European Medicines Agency
SUV	Standardized uptake value	PMPA	2-phosphonomethylpentanedioic acid
DOTA	1,4,7,10-tetraazacyclododecane-1,4,7,10-tetraacetic acid	NIR	Near-infrared (NIR) fluorescence
		MOR	$\mu$ -opioid receptor
		DOR	$\delta$ -opioid receptor

positions, respectively; this flexibility likely contributes to a less stringent substrate specificity within the S1 site of the enzyme compared to the S1' site, thus modulating the affinity of GCPII inhibitors. The formation of this pocket is allowed by the simultaneous positioning of Arg536 into the "binding" configuration and Arg463 into the "up" position [7,8].

The structural freedom provided by the S1 pocket has been exploited for the development of imaging probes for prostate cancer.

In the last few years, several radiotracers have appeared in many clinical trials for the diagnosis and treatment of prostate cancer, with radioligand-imaging, radioligand-therapy or surgery-radioguided objective [4], overcoming radiolabelled choline derivatives and [ $^{18}\text{F}$ ] DCFBC ( $^{18}\text{F}$ -Fluciclovine or Axumin) (Fig. 2) for recurrent disease with low PSA levels [9].

Considering the abundance of PSMA-based probes appeared in the literature till now, this paper points the attention on radiopharmaceuticals with increasing clinical application.

## 2. $^{18}\text{F}$ labeled compounds: [ $^{18}\text{F}$ ] DCFPyL, [ $^{18}\text{F}$ ] PSMA 1007 and [ $^{18}\text{F}$ ] PSMA JK-7 in clinical practice

The search for increased uptake within the tumour cell allows to obtain improved imaging quality and rapid renal excretion combined with low background activity. This aspect prompted researchers to focus on low-molecular weight  $\alpha$ -NAAG-based compounds. Radiopharmaceuticals such as [ $^{18}\text{F}$ ]FDCfYL, [ $^{18}\text{F}$ ]PSMA-1007, [ $^{18}\text{F}$ ]PSMA-JK-7, [ $^{68}\text{Ga}$ ]PSMA, [ $^{177}\text{Lu}$ ]PSMA-617, [ $^{99\text{mTc}}$ ]PSMA have been selected due of their features as the most promising in the current landscape of Nuclear Medicine. They permit to improve the accuracy of Pca tumour detection in terms of sensitivity and specificity, although some limitations remain regarding pharmacokinetics and detection rates in patients with very low PSA values (<1 ng/mL). This is lower than the

conventional imaging, with a significant clinical impact, since early salvage radiotherapy and surgery of local disease offer a chance of cure.

Historically, the first PSMA-targeted radiopharmaceuticals were based on conjugation of the ligand with gallium-68 and had some limitations in use, which were later overcome with the advent of fluoride- $^{18}\text{F}$ -based radiopharmaceuticals.

The two most studied fluoride-18 radiolabeled PSMA ligands recently introduced in the clinical practice in patients with biochemical recurrence or progression of prostate cancer (PC) by multiparametric PET/CT (dynamic and total body) are [ $^{18}\text{F}$ ]DCFpYL (or 2-(3-{1-carboxy-5-[(6-[ $^{18}\text{F}$ ]fluoro-pyridine-3-carbonyl)-amino]-pentyl)-ureido)-pentanedioic acid) and [ $^{18}\text{F}$ ]PSMA-1007 (((3S,10S,14S)-1-(4-(((S)-4-carboxy-18 2-((S)-4-carboxy-2-(6- Fluoronicotinamido) butanamido) methylphenyl)-3-(naphthalen-2-methyl)-1,4,12-trioxo-2,5,11,13-tetrazaadecane-10,14,16-tricarboxylic acid)) [10].

First-generation fluorine-18 radiolabeled PSMA ligands include [ $^{18}\text{F}$ ] DCFBC or [ $^{18}\text{F}$ ]Fluciclovine, a synthetic amino acid (amino-3-[ $^{18}\text{F}$ ]urocyclobutane carboxylic acid), which is carried by multiple sodium-dependent and sodium-independent channels up regulated in Pca cells. The main use indication of this PET radiopharmaceutical approved in both USA and Europe, involves the detection and localization of Pca recurrence in patients with increasing PSA after previous therapy. The primary advantages of  $^{18}\text{F}$ -Fluciclovine lie in its low urinary excretion, which allows better assessment of the prostate bed and reduced uptake into inflammatory cells (e.g., macrophages) [2].

$^{18}\text{F}$ -PSMA-1007, a second-generation radiopharmaceutical based on the radiopharmaceutical-PSMA interaction, appears to be the most advantageous among other candidate  $^{18}\text{F}$ -PSMA ligands because it demonstrates high radiolabeling yield, improved cancer uptake and non-urinary clearance. It was recently introduced into clinical practice after successful preclinical studies.

$^{18}\text{F}$ -PSMA-1007 PET/CT imaging appears to be very promising for

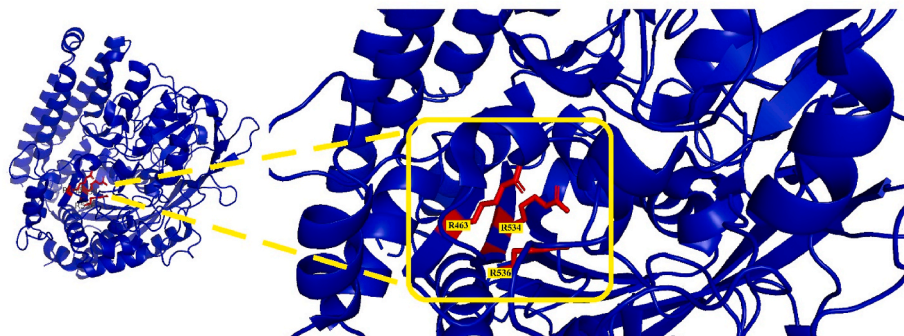


Fig. 1. Molecular structure of prostate-specific membrane antigen, with a particular detail of the S1' cationic side chain, consisting of the triad Arg534, Arg536 and Arg 463.

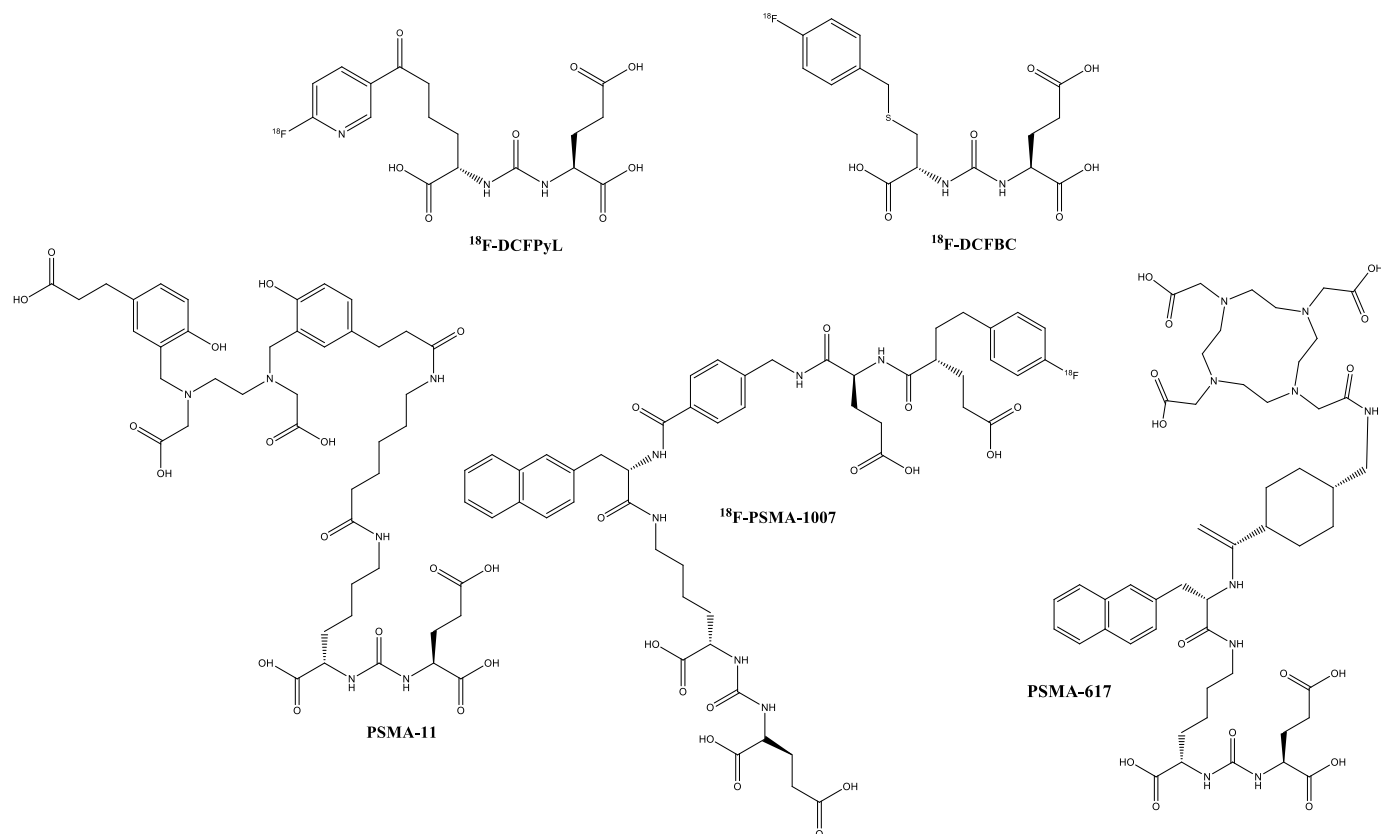


Fig. 2. Comparison of different PSMA ligands.

staging and restaging patients with PCa, especially when biochemical recurrence is under investigation. Regarding its use, it seems to work better than other imaging modalities such as bone scintigraphy, <sup>18</sup>F-FDG PET/CT or <sup>18</sup>F-Choline PET/CT, but its high cost and low availability should be taken in consideration [2]. The usual distribution of the radiotracer, which mainly includes the liver and gallbladder due to hepatobiliary clearance, allows for low background relatively to the spleen, pancreas, submandibular, sublingual, lacrimal and parotid glands, kidneys, urinary glands, bladder and small intestine, quantifying the maximum standardized uptake value (SUV max) for each lesion [2].

[<sup>18</sup>F] DCFPyL, the lead compound of PSMA-targeted radiopharmaceuticals, has been appreciated for its clear imaging and ability to reduce pre-acquisition waiting time due to its hydrophilicity and thus rapid renal excretion [11].

[<sup>18</sup>F]DCFPyL is as effective as <sup>68</sup>Ga-PSMA-11, while showing advantages intrinsic to fluorinated radiopharmaceuticals (e.g., large-scale productions) [12].

Similarly to [<sup>68</sup>Ga] PSMA-11, [<sup>18</sup>F]DCFPyL is rapidly eliminated by renal excretion and thus also shows rapid onset of activity in the ureters and bladder [4].

In spite of excellent image quality with both tracers, a significantly high uptake with [<sup>18</sup>F]DCFPyL was found in the kidneys, urinary bladder and in the lacrimal glands. In contrast, a significantly high uptake of [<sup>18</sup>F]PSMA-1007 was found in muscle, submandibular and sublingual glands, spleen, pancreas, liver and gallbladder [4].

Moreover, due to these different metabolization and excretion processes, radiopharmaceuticals could have specific uses. Non-urinary excretion of [<sup>18</sup>F]PSMA-1007 could aid clinical decision making in local recurrence and pelvic lymph node metastasis, while due to its slightly increased lipophilic characteristics, <sup>18</sup>F-PSMA-1007 is mainly eliminated through the hepatobiliary excretion pathway resulting in enhanced gallbladder and intestinal accumulation, compared with [<sup>18</sup>F] DCFPyL or <sup>68</sup>Ga-PSMA-11, therefore, the lower hepatic background of

[<sup>18</sup>F]DCFPyL and <sup>68</sup>Ga-PSMA-11 might promote these tracers in rare cases of advanced stage with liver metastasis [4].

Feeding of PCa patients by either fasting or drinking high-calorie beverages in order to reduce liver activity did not result in any significant effect on the absorption of <sup>18</sup>F-PSMA-1007 in the liver or small intestine [13].

An interesting result regarding the distribution of radiopharmaceuticals was obtained from semi quantitative image analysis. <sup>18</sup>F-PSMA shows higher uptake in lymph node metastases than in bone metastases, which may reflect a difference in the tumour biology of these types of metastases regarding PSMA expression [10].

Overall, the substantial uptake of <sup>18</sup>F-PSMA-1007 was associated with greater primary PC aggressiveness. Compared with other radiological and scintigraphic imaging methods, [<sup>18</sup>F]PSMA 1007 PET/CT showed superior sensitivity in detecting metastatic disease, while, when compared with other PSMA-targeted PET/CT tracers, it showed similar results in terms of diagnostic accuracy for staging PCa, an imaging approach that is still more effective than bone scintigraphy and conventional abdominal imaging.

Dual imaging with multiparametric MRI and <sup>18</sup>F-PSMA-1007 PET/CT, combined with final histopathological examination, could improve staging of primary PCa. In particular, <sup>18</sup>F-PSMA-1007-PET/CT can detect metastatic disease in a significant number of patients with negative standard imaging.

So, the <sup>18</sup>F-PSMA-1007 PET/CT provides accurate primary staging of PCa (*T-staging*); for lymph node staging (*N-staging*), it can detect lymph node metastases of PCa, even small ones, with high specificity, while for the detection of distant metastases of PCa (*M-staging*), the accuracy of <sup>18</sup>F-PSMA-1007 PET/CT for detecting bone metastases was superior than bone scintigraphy (with planar and tomographic acquisitions), CT and full-body MRI [13].

Therefore, <sup>18</sup>F-PSMA-1007 PET/CT is particularly effective for the purpose of establishing the most appropriate treatment modality and

just as reliable in order to avoid any unnecessary or harmful intervention.

This finding could have its clinical translation in the field of *radiothera(g)nostics* and, in particular, in the potential use of  $^{18}\text{F}$ -PSMA-1007 PET/TC for screening patients with lesions that exhibit high affinity for radiotracer binding and internalization in cancer tissue [10].

These patients would be suitable candidates for targeted therapies with vectors for PSMA, using therapeutic nuclides such as  $^{177}\text{Lu}$   $\beta$ -emitting or  $^{225}\text{Ac}$   $\alpha$ -emitting, which using a chelating system, such as the 1,4,7,10-tetraazacyclododecane-1,4,7,10-tetraacetic acid (DOTA) of PSMA-617, could be incorporated into PSMA-targeted vectors. In the just-described vector class, PSMA-617, a vector that combines a selective structure for PSMA with a DOTA chelating system, was chosen as the lead structure [14].

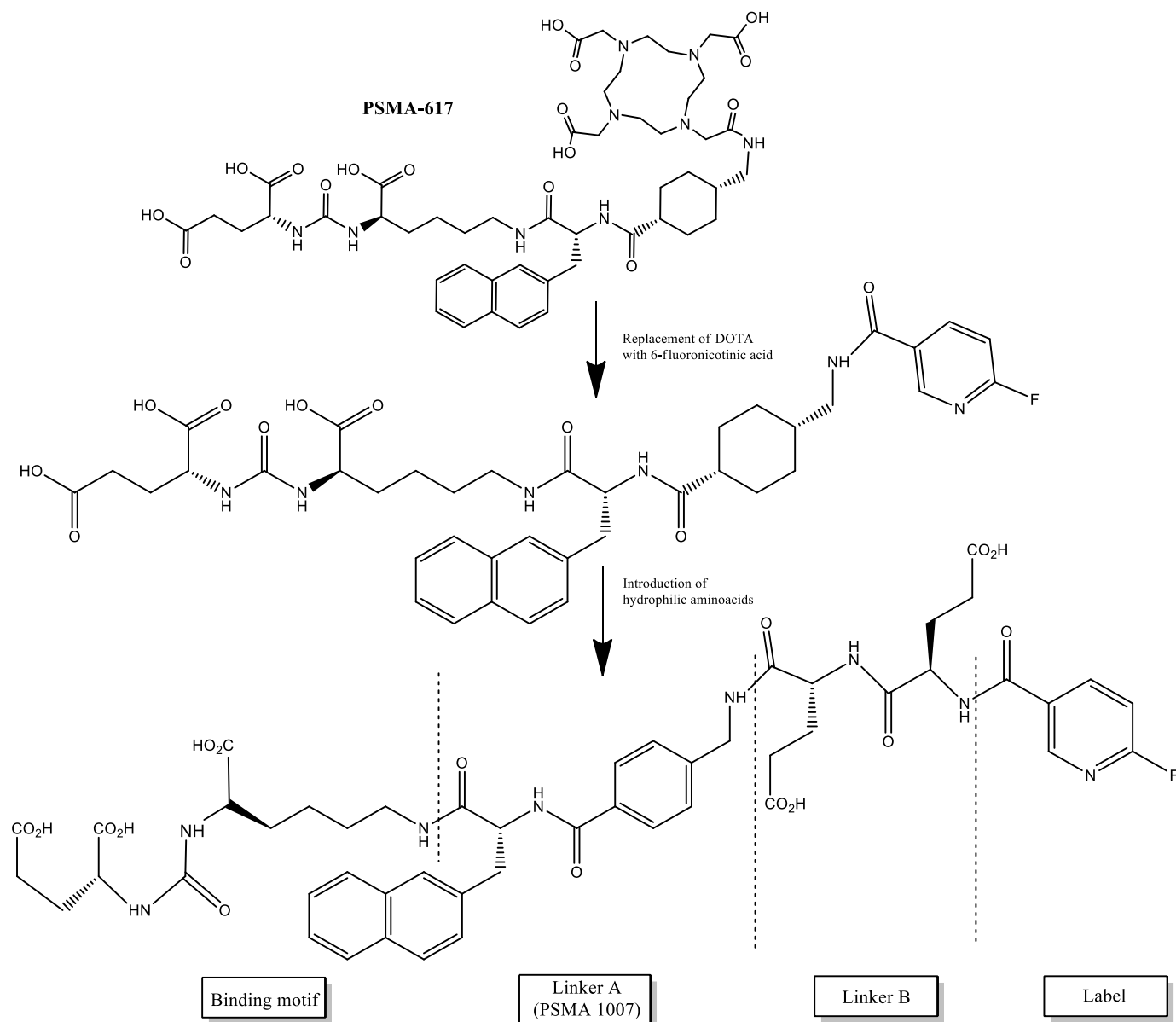
Starting from this compound, new solutions could be developed. Scheme 1 summarizes the synthesis steps. The acid chelator was replaced by fluoronicotinic acid to allow easy introduction of Fluoro-18 into the molecule. During the development stages of PSMA-617, it was already known that hydrophobic amino acids in the linker played a

critical role in the affinity and uptake of PSMA ligand [14].

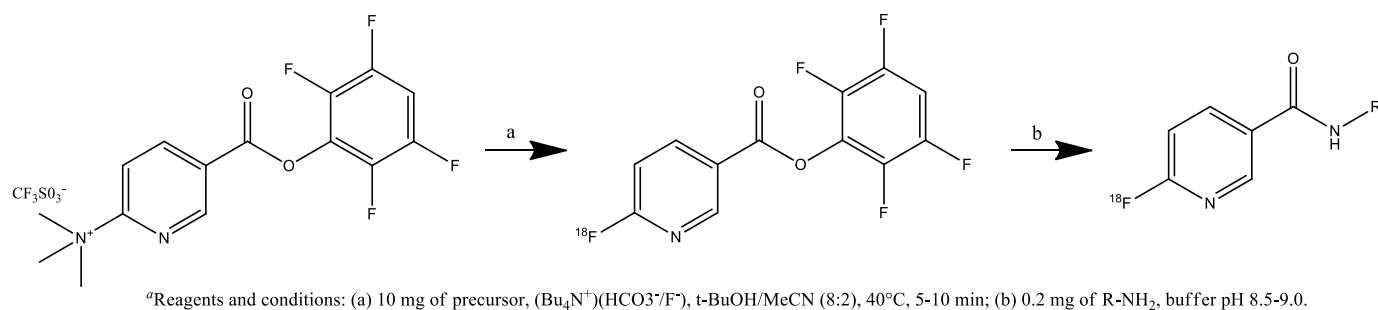
Therefore, only minimal changes in this area were considered. However, it was found how the replacement of DOTA with 6-fluoronicotinic acid and the consequent loss of hydrophilicity had a negative impact on biodistribution. For these reasons, additional hydrophilic amino acids were added to the linker, leading to the development of [ $^{18}\text{F}$ ]PSMA-1007, which has been successfully translated into the clinic and it is now undergoing advanced clinical studies.

The introduction of Fluoro-18, on the other hand, was carried out using a two-step procedure through the intermediate 6- [ $^{18}\text{F}$ ]Fluoronicotinic acid 2,3,5,6-tetrafluorophenyl ester ([ $^{18}\text{F}$ ]F-Py-TFP, Scheme 2) [15], because of its rapidity and simplicity [14].

Among other  $^{18}\text{F}$ -labeled derivatives that target PSMA,  $^{18}\text{F}$ -JK-PSMA-7, developed by the Jülich/Köln group (Research Center Jülich and University Hospital Cologne), has a structure that differs from that of DCF-PyL for the presence of a methoxy group on the fluoropyridine ring (Fig. 3) [16]. JK-PSMA-7 was recently successfully tested in two clinical trials in patients with biochemical recurrent prostate cancer, performed on a standard analogue PET/CT and used as a comparison to



Scheme 1. Key steps in the development of the [ $^{18}\text{F}$ ] PSMA 1007 and the link structure.



**Scheme 2.** Procedure for radiolabeling from [<sup>18</sup>F]-F-Py-TFP<sup>a</sup>.

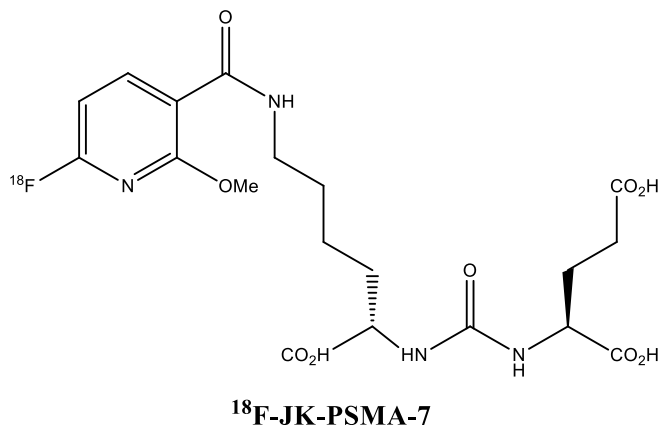


**Fig. 3.** Molecular structure of [<sup>18</sup>F]JK-PSMA-7.

evaluate the efficacy of <sup>18</sup>F-JK-PSMA-7 detection in patients with BCR on digital PET/CT with an adapted imaging protocol [17–20].

<sup>18</sup>F-JK-PSMA-7 demonstrated higher cell-specific uptake of PSMA than <sup>18</sup>F-DCFPyL. Although the target/background ratios of <sup>18</sup>F-DCFPyL and <sup>18</sup>F-PSMA-1007 were comparable, this parameter was high for <sup>18</sup>F-JK-PSMA-7 and low for <sup>68</sup>Ga-PSMA-11 [21].

The imaging was more qualitatively defined with <sup>18</sup>F-JK-PSMA-7 and <sup>18</sup>F-PSMA-1007 than with <sup>18</sup>F-DCFPyL and <sup>68</sup>Ga-PSMA-11, the imaging resolution similar for all 4 tracers, while <sup>18</sup>F-PSMA-1007 demonstrated significantly higher protein binding to blood and bone uptake than the other tracers.

The effective dose of [<sup>18</sup>F]JK-PSMA-7 to the total body was estimated to be 1.09E-02 mGy/MBq. The highest radiation dose was observed in the kidneys (average 1.76E-01 mGy/MBq), followed by the liver (average 7.61E-02 mGy/MBq), salivary glands (average 4.75E-02 mGy/MBq), spleen (average 1.89E-02 mGy/MBq) and lungs (1.10E-2 mGy/MBq) [18].

For [<sup>18</sup>F]JK-PSMA-7, a statistically comparable time of residence to [<sup>18</sup>F]PSMA-1007 was observed for the examined organs, being significantly higher in the liver and salivary glands, while no substantial difference was observed for kidney and spleen. In contrast, when comparing [<sup>18</sup>F]JK-PSMA-7 and [<sup>18</sup>F]-DCFBC in kidneys and liver, the time of residence was high for [<sup>18</sup>F]-JK-PSMA-7 and comparable in spleen and lungs [18].

Regarding the residence times of the tracer in the various organs, no significant difference was found between [<sup>18</sup>F]JK-PSMA-7 and [<sup>18</sup>F]-PSMA-1007; instead, significant increase was found for liver compared with DCFBC and DCFPyL [18].

[<sup>18</sup>F]JK-PSMA-7 showed rapid excretion through the blood analogously to [<sup>18</sup>F]-DCFPyL, unlike [<sup>18</sup>F]-PSMA-1007 and [<sup>68</sup>Ga]-PSMA-11, whereby protein binding in the blood was high, delaying tracer excretion and reducing accumulation in the kidneys and bladder. This could

be advantageous for detecting PCa metastasis adjacent to the urethra and bladder, while a fast excretion would decrease background noise and improve imaging quality [18].

In the study above, conducted on ten patients with prostate cancer and biochemical recurrence or radiologic evidence of metastatic diseases, the time course of SUV (Standardized Uptake Value) values was analysed not only for organs but also for <sup>18</sup>F-PSMA-positive lesions over a long period of time. The SUV max and peak SUV values in PSMA-positive lesions increased up to 60 min p.i. and remained so in subsequent PET/CT scans up to 140 min p.i. It was thus possible to deduce that a prolonged acquisition time window, even up to 3 h after injection, is also favourable for this tracer.

This confirms the evaluations resulting from Lu<sup>177</sup>-PSMA-based therapies, namely, how uptake of the tracer in PSMA-positive lesions increased up to 24 h after injection, while uptake in no target organs peaked on the day of treatment and then decreased thereafter, for these reasons, there might be a clear advantage over [<sup>68</sup>Ga]-PSMA-11 [18].

In view of the above, <sup>18</sup>F-JK-PSMA-7 appears to be a promising candidate for high-quality visualization of small PSMA-positive lesions. The excellent preclinical imaging properties justify further preclinical and clinical studies of this tracer.

### 3. Gallium-68 against Fluorine-18, as a radioisotope

Over the past two decades, radionuclide diagnosis and therapy have become increasingly popular in various clinical applications, despite the critical issues related to the choice of a radionuclide and its nuclear, chemical and biochemical characteristics, such as half-life, reactivity and especially stability in coordination structures or covalent bond strength [22].

In the diagnostic field, Gallium-68-based radiopharmaceuticals, one among them <sup>68</sup>Ga-PSMA-11, have shown significant clinical value in both biochemical recurrence of PC and primary staging [10], although they have some critical shortcomings, such as limited production capacity by *in situ* <sup>68</sup>Ge/<sup>68</sup>Ga generators, compared with production capacity by cyclotron and consequent reduced availability [14].

In addition, other disadvantages with which the use of Ga<sup>68</sup> as a radioisotope must contend include a relatively short half-life of 68 min for Ga<sup>68</sup>, compared with 109.8 min for F<sup>18</sup>, a limiting factor for both the delivery of Ga<sup>68</sup>-labeled PET tracers to other centres and delayed imaging. In addition, the Ga<sup>68</sup> positron energy is higher (1.90 MeV) than that of F<sup>18</sup> (0.65 MeV), decreasing the maximum theoretical spatial resolution and the capability to detect small and tightly spaced lesions in close proximity to each other [11].

However, the capacity to produce Gallium-68, using a commercially available generator, facilitates its application in PET centres without a cyclotron. The Gallium-68 produced by the generator is directly available for radioactive labelling using lyophilized kit formulations, but the production capacity only allows scanning in a limited number of patients depending on the lifetime of the generator itself. In contrast, Fluorine-18 produced by the cyclotron offers a wide range of radioactivity, ranging from a few tens to a few hundred GBq, which allows high

doses to be generated per single production run, as well as commercial distribution over long distances to satellite centres, removing the need for on-site radiolabeling [16].

Due to the steady growth in demand for PCa diagnostic examinations, in recent years there has been increasing interest in the development and introduction into clinical practice of radiofluorinated PSMA ligands, which, regardless of their biological characteristics, have the potential to make diagnostic examination easily accessible even for high incidences.

In addition, since the F-18 has a shorter positron range, a higher positron yield and a higher detection sensitivity, even of small tumor lesions, than Ga-68, efforts to take advantage of the isotopic characteristics of  $^{18}\text{F}$  for PSMA imaging led to the development of  $^{18}\text{F}$ -DCFPyL as the first  $^{18}\text{F}$ -based PSMA tracer [23].

#### 4. PSMA radiolabels used in theranostics ( $^{177}\text{Lu}$ -PSMA 617 for Vision study)

As previously discussed, prostate-specific membrane antigen (PSMA) is a promising target for imaging and targeted radionuclide therapy of prostate cancer and its metastases. The encouraging response rates and low toxicity profile of radioligand therapy (RLT) of metastatic castration-resistant prostate cancer (mCRPC), in this case  $^{177}\text{Lu}$ -labeled ligands, are increasingly evident.

This therapeutic approach is possible using low-molecular weight, radioligands characterized by high affinity for PSMA and rapid build-up in the cancer, e.g. PSMA-617 and PSMA I&T.

Both PSMA ligands have been successfully used in the clinic for the treatment of mCRPC by labeling with Lutetium-177, a  $\beta^-$ -emitting radionuclide ( $T_{1/2} = 6,65$  d;  $E\beta^-_{av} = 134$  keV, average path length = 0,7 mm-1,8 mm) being able to release beta energetic particles that destroy cancer cells at the disease site [24].

The first PSMA-targeted radioligand labeled with  $^{177}\text{Lu}$  was successfully made at Bad Berka in April 2013 [25]. Since DOTAGA allows equally efficient radiolabeling with  $\text{Ga}^{68}$ , this first PSMA-based compound with theranostic activity was named PSMA I&T (Imaging and Therapy) (Fig. 4), used in several centres, both for imaging with  $\text{Ga}^{68}$  and for radioligand therapy (RLT) with  $^{177}\text{Lu}$  [4].

At the same time, considering preclinical data (affinity, internalization rate) and biodistribution data in mice with LNCaP tumor (LN =

lymph nodes), PSMA-617 was selected as the most promising agent. Compared with  $^{177}\text{Lu}$ -PSMA I&T,  $^{177}\text{Lu}$ -PSMA-617 showed significantly low uptake in mouse kidneys, while tumour uptake and overall biodistribution in mice were similar [4].

Even if this aspect has often been considered as an important criterion and dosimetric advantage in subsequent studies in humans, a direct comparison of both tracers in patients demonstrated quite identical renal clearance kinetics of  $^{177}\text{Lu}$ -PSMA I&T and  $^{177}\text{Lu}$ -PSMA-617 [4].

In 2015, a multicenter retrospective clinical trial of 145 patients with a total of 248 therapeutic cycles started to evaluate the efficacy and safety of  $^{177}\text{Lu}$ -PSMA-617 in patients with metastatic prostate cancer mCRPC [26]. The study demonstrated favourable safety and high efficacy, superior to other systemic therapies in comparable patient cohorts [4].

Based on these promising clinical data, a global Phase III clinical trial (VISION) was undertaken in October 2017 with  $^{177}\text{Lu}$ -PSMA-617 in men with mCRPC. This study led to Pluvicto (Lutetium Lu-177 vipivotide tetraxetane) being approved by the FDA, in March 2022 [27–29], in the United States, Great Britain and Canada and by the EMA (Committee for Medicinal Products for Human Use) in October 2022 for all 27 European Union member states, as well as Iceland, Norway, Northern Ireland and Liechtenstein [30] (Fig. 5).

These PSMA-targeting ligands share a similar molecular structure with three components: (1) the urea-glutamic acid group (-Lys-NH-CO-NH-Glu), which binds to the PSMA pocket, (2) a linker and (3) a metal complex, a region that carries radioactive isotopes for imaging or radionuclide therapy (Fig. 5). This structure has the property of delivering the radiopharmaceutical to the selected area and can be used if labeled with Gallium-68 in diagnostics and with Lutetium-177 for therapy [31]. The proper combination of these three components leads to successful PSMA targeting agents, as they consist of a solid structure that is well adapted to optimize radionuclide activity, drug binding affinity and *in vivo* properties for imaging or radioligand therapy (RLT) [31].

Therefore, in light of the encouraging response rates that are more and more evident and the low toxicity profile of radioligand therapy, PSMA-based imaging and RLT, especially with  $^{177}\text{Lu}$ -PSMA-617, are promising and currently applied therapeutic approaches in the treatment of metastatic castration-resistant PC.

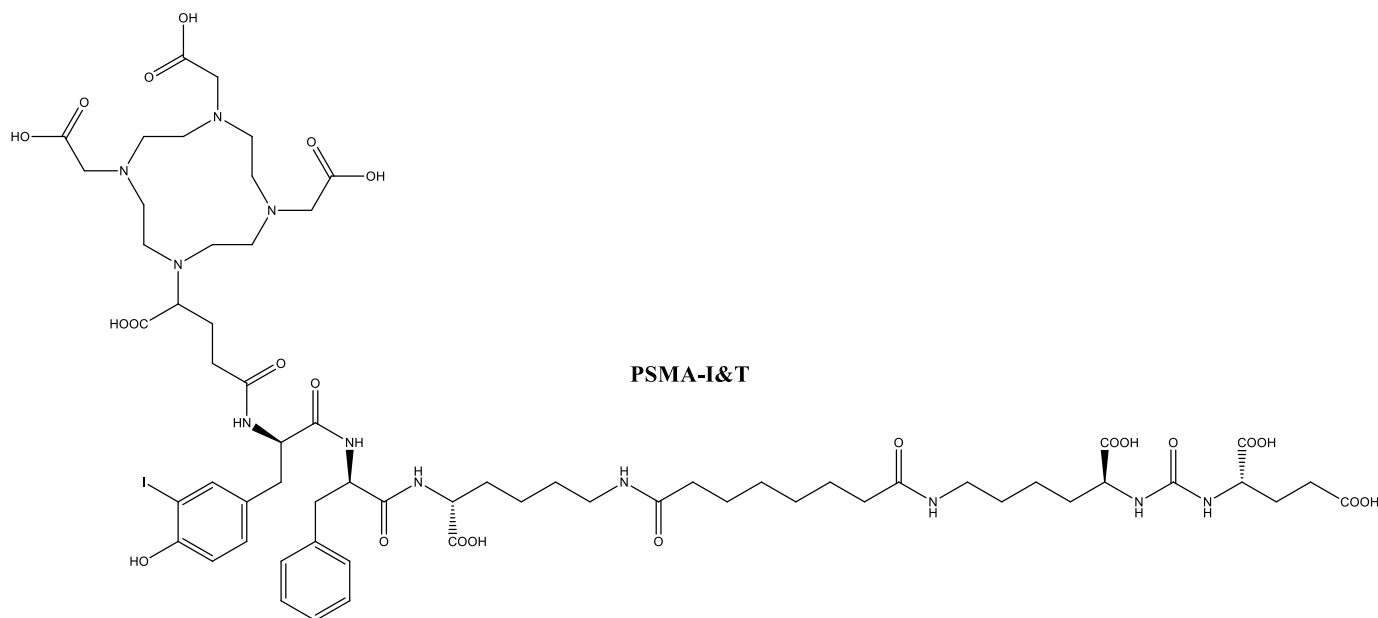


Fig. 4. Molecular structure of PSMA I&T, the first RLT precursor.

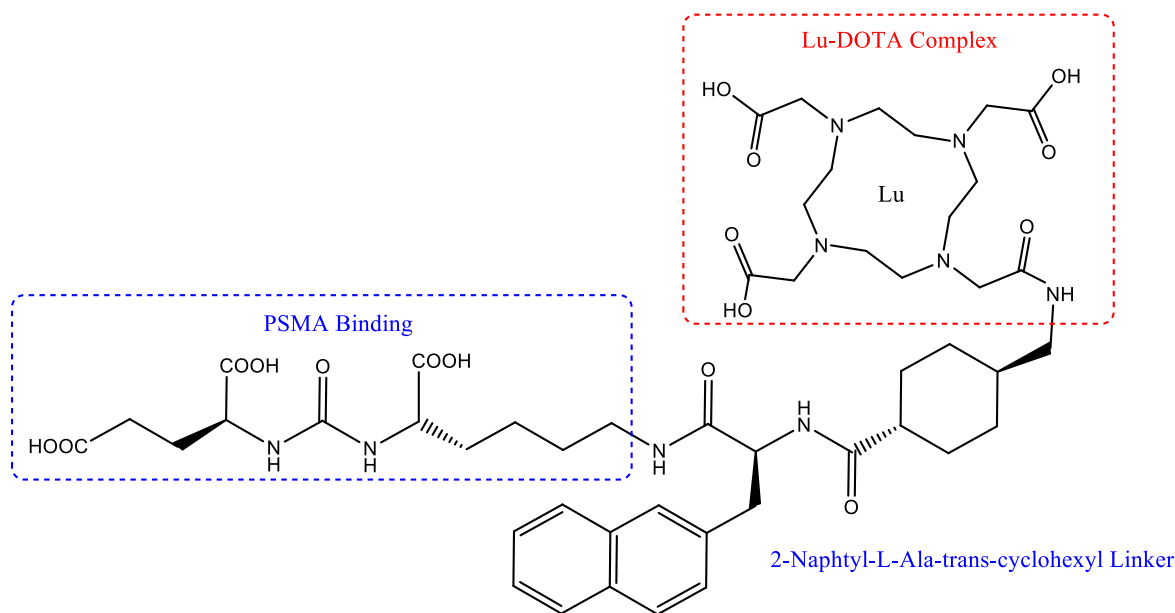


Fig. 5. [ $^{177}\text{Lu}$ ]Lu-PSMA 617 Pluvicto<sup>TM</sup> (Lutetium (Lu-177) vipivotide tetraxetan).

### 5. [ $^{18}\text{F}$ ] AIF-PSMA approach

Unfortunately, Fluorine-18-based radiopharmaceuticals have optimal characteristics as regards the imaging but cannot be translated as such into therapy and this implies high equivalence studies for dual use. For this reason, the aluminium fluoride species  $^{18}\text{F}\text{-AIF}$  has been developed in the direct labelling of PSMA ligands with a radiometallic chelating system, which allows it to be compared to a radiometallic ion and thus incorporated into the coordination system. This method provides a simple and freely accessible way for the synthesis of PET imaging  $^{18}\text{F}$ -labeled agents [32].

Gallium-68 continues to be an attractive radioisotope for radiopharmaceutical development because of the simple and rapid synthetic procedures and kit formulations available [16,33–35]. Due to its

metallic nature, Gallium-68 is incorporated into a radioligand using a chelator through coordination chemistry. The most commonly used chelators are polyaminocarboxylated macrocycles, such as 1,4,7,10-tetraazacyclododecane-1,4,7,10-tetraacetic acid (DOTA), 1,4,7-triazacyclododecane-1,4,7-triacetic acid (NOTA), N,N'-bis-[2-hydroxy-5-(carboxyethyl)benzyl] ethylenediamine-N,N'-diacetic acid (HBED-CC) (Fig. 6).

However, due to more favourable imaging characteristics of Fluorine-18 than Gallium-68, a new technique was developed for introducing Fluorine-18 into a biomolecule through metal-based radiochemistry.  $\text{Al}^{3+}$  is a trivalent metal with gallium-like ionic radius, it has the capacity to bind to fluorine stably, forming the fluorine-aluminium complex ( $\text{AlF}^{2+}$ ) with high stability *in vivo*. In this new form,  $\text{AlF}^{2+}$  can form stable complexes with hexadentate ligands such as

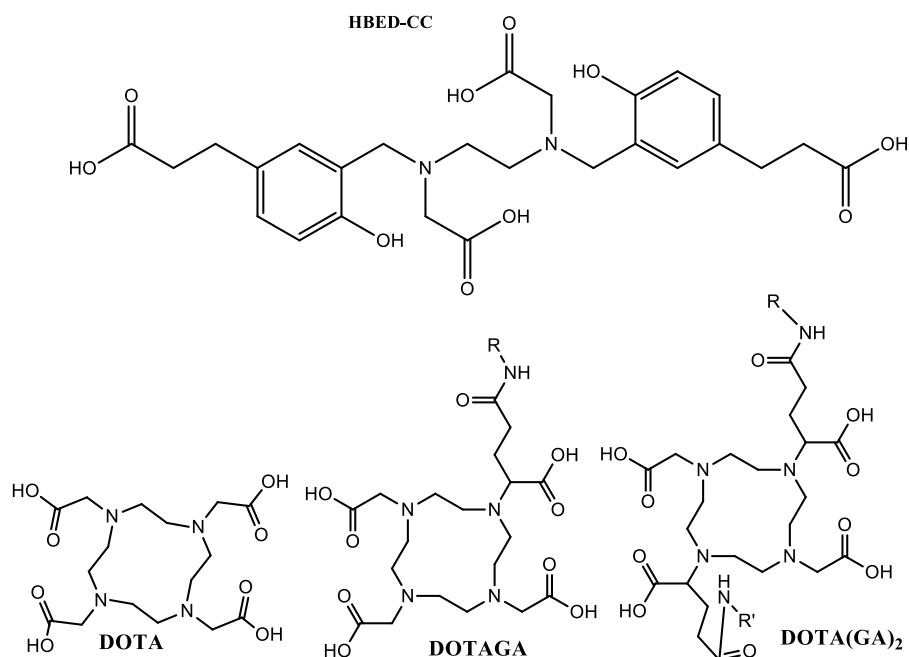


Fig. 6. Chelation agents able to complex therapeutic radionuclides.

NOTA or HBED-CC [16].

McBride et al. demonstrated the feasibility of an  $^{18}\text{F}$  radiolabelling method by complexing  $\text{AlF}^{2+}$  with a chelator NOTA, bound to a peptide [36,37]. PSMA-11 (or PSMA-HBED-CC), a ligand successfully applied to the formulation of radiopharmaceuticals, has been used as a starting point for the preparation of an analogous radiopharmaceutical based on a chelating system for AlF. The success of previous radiofluorination of peptides by complexation with  $\text{AlF}^{2+}$  has paved the way for the development of  $^{18}\text{F}$ -AlF-PSMA-11 (Fig. 7).

*In vitro*,  $^{18}\text{F}$ -AlF-PSMA-11 demonstrated high tumour uptake, expressed as %ID, *i.e.*, percentage of injected dose, in PSMA-LS174T cells, which was almost comparable to that of the equivalent  $\text{Ga}^{68}$ -labeled compound; in fact, a % ID/g of  $10.8 \pm 2.3$  % and  $7.9 \pm 1.3$  % ID/g was recorded for the fluorinated compound and for the  $\text{Ga}^{68}$ -labeled compound, respectively, at 2 h after injection, while the uptake of renal activity at 2 h after injection was higher for  $^{68}\text{Ga}$ -PSMA-11 ( $105.8 \pm 13.8$  % ID/g) than for  $^{18}\text{F}$ -AlF-PSMA-11 ( $43.5 \pm 5.7$  % ID/g). Both radiotracers demonstrated rapid and similar internalization rates [38].

Biodistribution studies in mice revealed high retention in the kidneys and bladder; this could be due to renal excretion of the radiotracer and its specific binding to PSMA-expressing mouse kidneys [39,40].

The internalization profile of  $^{18}\text{F}$ -AlF-PSMA-11 and the reference compound  $^{68}\text{Ga}$ -PSMA-11, was also evaluated and compared to assess whether the lack of stability could affect the internalization capacity of

$^{18}\text{F}$ -AlF-PSMA-11: after 30 and 60 min, they were found to be almost similar, while the internalization of  $^{68}\text{Ga}$ -PSMA-11 was significantly higher than that of  $^{18}\text{F}$ -AlF-PSMA-11 after 120 min [38].

A dosimetry study for  $^{18}\text{F}$ -PSMA-11 in six PCa patients demonstrated rapid blood clearance and high urinary excretion ( $29.0 \pm 5.9$  % at 5 h p.i.). High uptake of the tracer was observed in the salivary and lacrimal glands, kidneys, bladder, spleen and liver at 20 min p.i. The mean effective dose was determined to be  $12.8 \pm 6$   $\mu\text{Sv}/\text{MBq}$ , with the highest radiation doses to the urinary bladder wall ( $126 \pm 3.27$   $\mu\text{Gy}/\text{MBq}$ ) and kidneys ( $85.0 \pm 16.4$   $\mu\text{Gy}/\text{MBq}$ ) [16,41].

A comparative study of  $^{18}\text{F}$ -AlF-PSMA-11 and  $^{68}\text{Ga}$ -PSMA-11 in 37 patients with BCR after primary treatment showed comparable diagnostic performance with 46 % positivity rates for  $^{18}\text{F}$ -AlF-PSMA-11 compared with 49 % for  $^{68}\text{Ga}$ -PSMA-11 [42].

Therefore,  $^{18}\text{F}$ -AlF-PSMA-11, as alternative to  $^{68}\text{Ga}$ -PSMA-11, emerges as an elegant solution to the need for an  $^{18}\text{F}$ -labeled PSMA ligand, since by the way it can be prepared from the same precursor, which is also widely available at low cost [43]. However, the rapid instability observed *in vivo* and subsequent uptake in bone indicate that this tracer requires extensive *in vitro* evaluation, before further pre-clinical or clinical studies can be initiated [44].

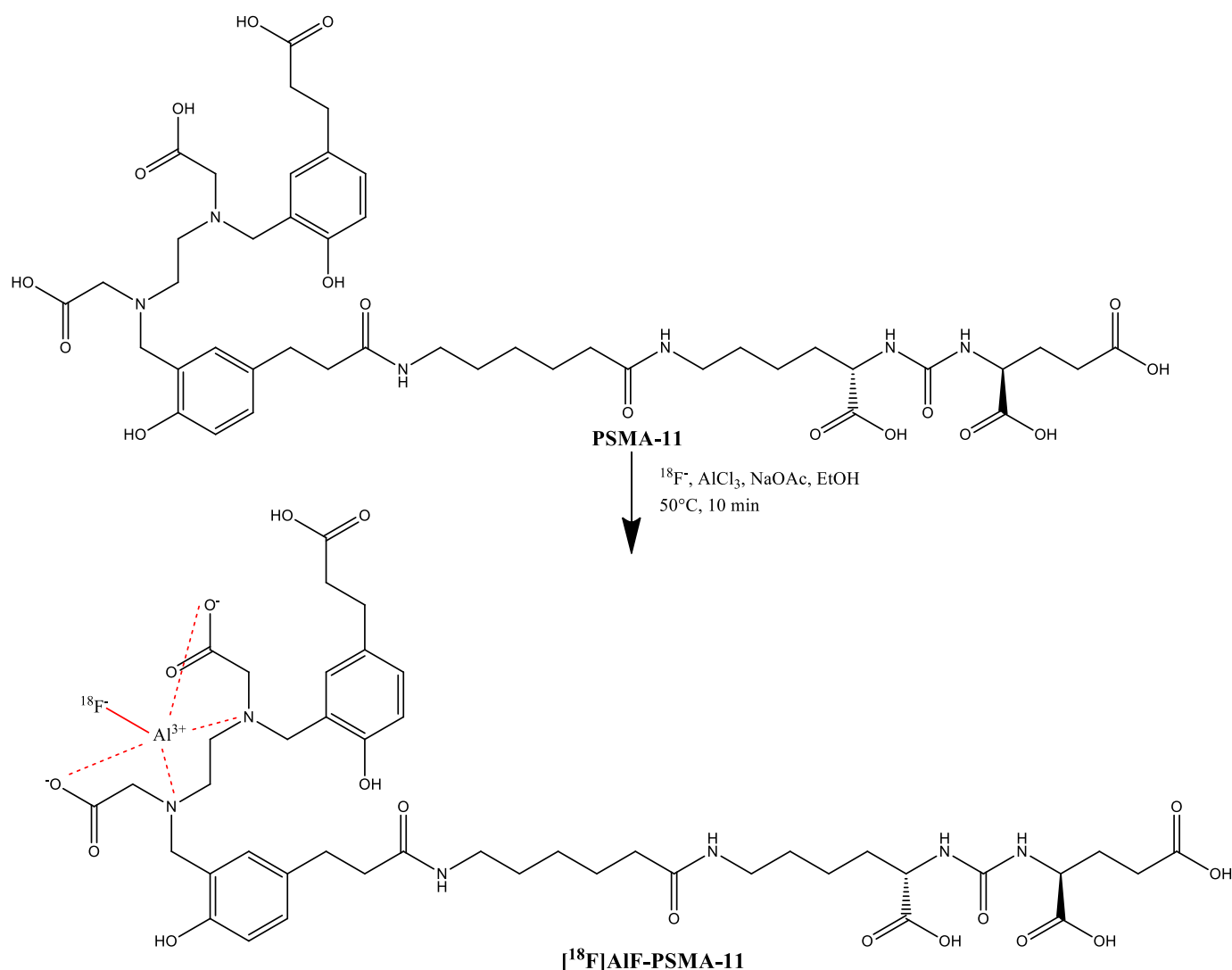


Fig. 7. Radiosynthesis of  $^{18}\text{F}$ -AlF-PSMA-11.

## 6. Discussion

In recent years, PSMA-PET/CT has been an innovative diagnostic approach for staging and follow-up of patients with PC recurrence, overcoming the challenges of low sensitivity and specificity of conventional imaging modalities [45].

In the overview of radiotracers used for diagnostic purposes,  $^{18}\text{F}$ -PSMA-1007 has garnered great interest in the clinical field, showing to be a viable alternative to the routine use of  $^{68}\text{Ga}$ -PSMA and more effective than other radiotracers available on the market, such as those based on choline [46] and  $^{18}\text{F}$ -fluciclovine [47] for patients with recurrent PCa. In fact, it shows a series of advantages, such as more extended physical decay compared with  $^{68}\text{Ga}$ -PSMA, the ability to study a large patient population each day, the relatively low excretion by the urinary system and the high tumor-to-background ratio [1,48,49].

By virtue of its marked lipophilicity and being excreted mainly by hepatobiliary clearance,  $^{18}\text{F}$ -PSMA-1007 on the one hand, could obscure the detection of small liver lesions [16], usually occurring in the later stage of the disease, but at the same time, it could allow an increased in accuracy interpretation of tumor lesions, even particularly tiny ones, located near regions affected by renal clearance [50].

In fact, considering how much of the PSMA tracers have hydrophilic character and renal clearance, measures to be used to reduce as much as possible the interference with the detection of small recurrent lesions near the urinary tract include emptying the bladder before scanning in combination with administration of a diuretic. This was mainly observed for [ $^{68}\text{Ga}$ ]PSMA-11 in which administration of furosemide increased the diagnostic confidence about the presence of PSMA-positive lesions [50,51].

Another important challenge for radioactive labeling with a fluoride-aluminum complex is the selection of the appropriate chelator: for [ $^{18}\text{F}$ ]AlF-PSMA-11, the chelator HBED-CC, also used for [ $^{68}\text{Ga}$ ]PSMA-11, was chosen; for [ $^{18}\text{F}$ ]AlF-PSMA-BCH and [ $^{18}\text{F}$ ]Bi-PSMA, NOTA was selected as the chelator to allow labeling with multiple radionuclides (gallium-68, fluorine-18, lutetium-177 ...).

Furthermore, in the evaluation of F18-labeled PSMA tracers, the gradual defluorination, which involves non-specific bone uptake and therefore interference in the detection of bone metastases, could represent a limiting factor, especially for delayed imaging, useful for the detection of lesions with low PSMA expression and slow accumulation of the radiotracer [50].

The previously mentioned PSMA ligands are also characterized by variable binding affinity. The [ $^{18}\text{F}$ ]DCFPyL has a relatively low binding affinity ( $\text{IC}_{50} = 12,3 \pm 1,2 \text{ nM}$ ), followed by [ $^{68}\text{Ga}$ ]PSMA-11 ( $\text{IC}_{50} = 5,2 \pm 0,9 \text{ nM}$ ), [ $^{18}\text{F}$ ]PSMA-1007 ( $\text{IC}_{50} = 4,2 \pm 0,5 \text{ nM}$ ), [ $^{18}\text{F}$ ]Bi-PSMA ( $\text{IC}_{50} = 4,1 \pm 0,4 \text{ nM}$ ) and [ $^{18}\text{F}$ ]CTT1057 ( $\text{IC}_{50} = 0,4 \text{ nM}$ ) [52–54].

However, these relatively small differences in binding affinity, which for most PSMA radiotracers are in the order of a few nanomolars, might be of greater interest for therapeutic ligands, since higher binding affinity would ensure greater internalization of the ligand, extending the residence time of the radioligand in the tumor cell.

Further investigation is needed as to whether the higher affinity may have a negative effect, potentially leading to more false-positive results.

With the aim to improve the radioligand-targeted therapy of metastatic prostate cancer and limit its undesirable effects as much as possible, some new therapeutic strategies are being investigated. In fact, to overcome salivary gland toxicity (xerostomia or dry mouth syndrome) considered as the main limitation of targeted  $\alpha$ -RLT treatment to date, scialendoscopy, intraparenchymal injections of botulinum toxin combined with other drugs or external cooling of salivary glands with ice packs are used with little success [4]. It appears that a potential cause of dry mouth after targeted  $\alpha$ -therapy is also the direct effect of radiation and not only the inflammatory process.

However, it has recently been reported that an intraperitoneal injection of monosodium glutamate is able to reduce the uptake of [ $^{68}\text{Ga}$ ]PSMA-11 in the salivary glands and kidneys of LNCaP tumor-bearing

mice (LNCaP cells are an experimental model experimental, used in vitro to study androgen-dependent prostate tumors), while leaving tumor uptake unaffected.

With the purpose of reducing PSMA inhibitor uptake in salivary glands and kidneys, specific PSMA inhibitors have been used as pre-treatment before administration of radiolabeled PSMA inhibitors (Fig. 8), such as 2-phosphonomethylpentanedioic acid (PMPA) and its orally available pro-drug (such as JHU-2545, for which both the phosphonate and a carboxylate are protected with isopropylloxycarbonyl methyl residues and *in vivo* release of 2-PMPA after oral administration has been demonstrated in both mice and dogs).

Increasing the binding of drugs to plasma proteins could be an effective strategy to reduce the clearance rate while improving the specific absorption of these drugs [55]. For this purpose, the conjugation of a low-molecular-weight domain or groups albumin-binding have been studied to enhance the tissue distribution of the corresponding bio-vectors [56]. As a result, the use of PSMA inhibitors, with increasing albumin binding and decelerated clearance kinetics, has been suggested as a promising approach to improve tumor uptake of therapeutic PSMA ligands.

With the goal of providing a molecular pattern that enables rapid and efficient radiolabeling of peptides and peptide-like radiopharmaceuticals, such as PSMA inhibitors with  $^{18}\text{F}$  or radiometals and that allows a single molecule to simultaneously provide diagnostic and therapeutic application, a new class of radiopharmaceuticals called radiohybrid PSMA ligands (rhPSMA) has recently been advanced, preclinically assessed and transferred into clinical trials. A unique property of rhPSMA ligands is their capacity to incorporate both covalently bound fluoride and a metal complex, with one of them alternatively radioactive and the other non-radioactive (for example, [ $^{18}\text{F}$ ][ $^{nat}\text{Ga}$ ]rhPSMA and [ $^{19}\text{F}$ ][ $^{68}\text{Ga}$ ]rhPSMA, or [ $^{18}\text{F}$ ][ $^{nat}\text{Lu}$ ]rhPSMA and [ $^{19}\text{F}$ ][ $^{177}\text{Lu}$ ]rhPSMA). For this reason, rhPSMA ligands can be exchangeable for PET imaging with both 18F and 68Ga, ensuring the tight correlation between pre-therapy imaging, dosimetry and/or monitoring with 18F and therapy with 177Lu [4].

Furthermore, it is interesting to observe that the most promising results were obtained by combining  $^{18}\text{F}$ -PSMA-1007 PET/CT and multiparametric MRI, suggesting a potential combination of these methods and thus an improvement in both PCa detection and local staging. In this regard,  $^{18}\text{F}$ -PSMA-1007 PET/MRI could be the future one-stop-shop imaging modality for PCa staging, although the availability of this method is still limited [57,58].

In the context of tumor-targeted imaging and therapy, peptide-based NIR fluorescent probes represent a valuable tools considering their high affinity and low toxicity [59].

In fact in the last 5 years most of researchers' efforts have been focalized in the design of nontoxic and efficacious "always-on" peptide-based NIR fluorescent probes; first attempts have been described on cyclic small peptides such as biphalin, which is a synthetic agonist of MORs and DORs (Fig. 9) [60–62].

A cyclic biphalin derivative, e.g. compound 17, has been promptly prepared using a side chain to side-chain-type cyclization between D-Pen/D-Cys residues and a fluorescein-dibromomaleimide linker [63]. It possesses a strong affinity for MOR and DOR and it is a potent MOR-/partial DOR agonist. This data indicate the possibility to consider biphalin as a scaffold for the future development of efficient fluorescent bioconjugates by using different probes and linkers [64]. Indeed, compound 1D results a fluorescent ligand, potentially useful as a labelling and imaging agent because it has a good separation between excitation and emission spectra, with the best affinity profile for MOR and DOR and ability to stimulate the G protein coupled receptors with high potency [64].

Such peptides could be applied in the fluorescence image-guided surgery, an emerging cancer therapy strategy aiming at achieve a precise tumor resection and tumor lesions recognition. However, most of these molecules rely on preclinical stage and require a deep

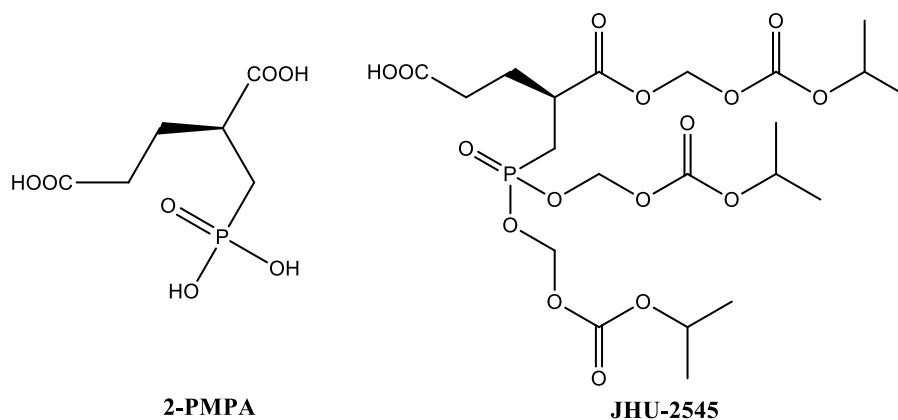


**Fig. 8.** PMPA, the PSMA inhibitor and the PMPA JHU-2545 pro-drug.

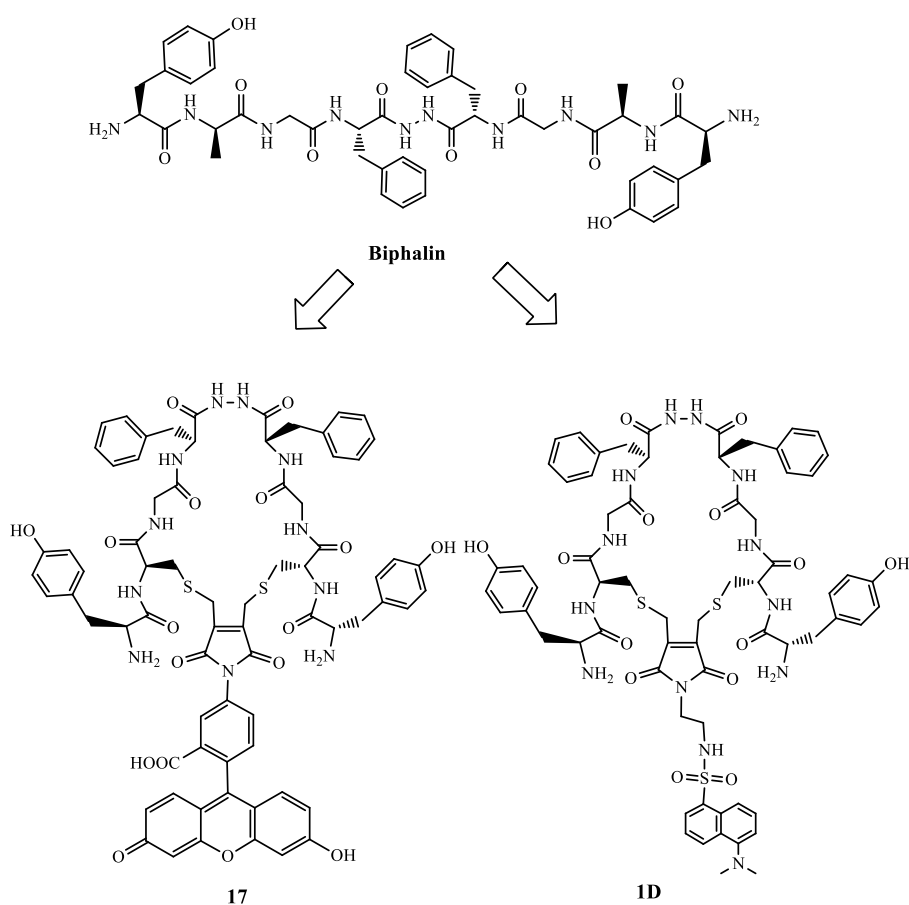


**Fig. 9.** Structures of biphalin and its fluorescent bioconjugates.

understanding of the signaling pathways in living organisms to bypass some physiological limitations and toxicity. Further investigation on pharmacodynamics and pharmacokinetic properties of these probes could potentiate the chances of clinical transformation, with social and economic benefits for the human wellbeing.

## 7. Conclusion

Overall, this systematic review highlighted the increasing diagnostic role of  $^{18}\text{F}$ -PSMA-1007 PET/CT in PCa staging [13].

In recent years, the development of PSMA-targeted tracers has

become one of the most active and dynamic fields of radiopharmaceutical research [4] and although the above-mentioned  $^{18}\text{F}$ -labeled PSMA PET tracers ensure good quality in image acquisition, each one of them shows both advantages and disadvantages in terms of radiosynthesis practicality, binding affinity, molecule stability, clearance, bio-distribution, etc.

In fact, the ideal PSMA-based tracer to be used for PET diagnosis should ensure a simple synthesis process, which results in high radiochemical purity, radiochemical yield and molar activity; in addition, uptake and accumulation at the receptor level should be rapid and highly specific, thanks in part to high binding affinity, thus ensuring

detection of small prostatic cancerous lesions while minimizing uptake in healthy organs, such as salivary glands, spleen and kidneys. In addition, rapid excretion of the drug from non-target tissues and the ability to label the molecule with both a diagnostic and therapeutic radionuclide, making it suitable for PSMA RLT, outline the ideal picture of the radiopharmaceutical par excellence [65,66].

Therefore, an improved diagnosis by PSMA PET, in combination with the choice of the most appropriate PSMA ligand and currently available cutting-edge instrumental technologies, could lead to improvements in the definition of the theranostic approach as well as an increasingly personalized and efficient RLT therapeutic strategy for staging high- and intermediate-risk PCA.

## Funding

This research did not receive any specific grant from funding agencies in the public, commercial or not-for-profit sectors.

## Author Contributions

**Giuseppe Capasso:** Methodology, Investigation, Resources, Formal analysis, Data curation, Writing – original draft. **Azzurra Stefanucci:** Formal analysis, Writing – review & editing. **Anna Tolomeo:** Methodology, Conceptualization, Supervision, Writing – review & editing, Project administration.

## Declaration of competing interest

The authors declare that they have no known competing financial interests or personal relationships that could have appeared to influence the work reported in this paper.

## Data availability

No data was used for the research described in the article.

## Acknowledgments

Thanks to Prof. Stefanucci for her support in the preparation of this review and Dr. Tolomeo for the opportunity to join the industrial PhD course at Department of Pharmacy, Università degli Studi “G. d’Annunzio” Chieti – Pescara, Italy.

## References

- [1] C. Maisto, A. Morisco, R. de Marino, et al., On site production of [18F]PSMA-1007 using different [18F]fluoride activities: practical, technical and economical impact, *EJNMMI radiopharm. chem.* 6 (2021) 36, <https://doi.org/10.1186/s41181-021-00150-z>.
- [2] N.K. Pianou, P.Z. Stavrou, E. Vlontzou, P. Rondogianni, D.N. Exarhos, I.E. Datsaris, More advantages in detecting bone and soft tissue metastases from prostate cancer using 18F-PSMA PET/CT, *Hellenic J. Nucl. Med.* 22 (1) (2019 Jan-Apr) 6–9, <https://doi.org/10.1967/s002449910952>. Epub 2019 Mar 7. PMID: 30843003.
- [3] A. Afshar-Oromieh, E. Avtzi, F.L. Giesel, T. Holland-Letz, H.G. Linhart, M. Eder, M. Eisenhut, S. Boxler, B.A. Hadaschik, C. Kratochwil, W. Weichert, K. Kopka, J. Debus, U. Haberkorn, The diagnostic value of PET/CT imaging with the (68)Ga-labelled PSMA ligand HBED-CC in the diagnosis of recurrent prostate cancer, *Eur. J. Nucl. Med. Mol. Imag.* 42 (2) (2015 Feb) 197–209, <https://doi.org/10.1007/s00259-014-2949-6>. Epub 2014 Nov 20. PMID: 25411132; PMCID: PMC4315487.
- [4] H.J. Wester, M. Schottelius, PSMA-targeted radiopharmaceuticals for imaging and therapy, *Semin. Nucl. Med.* 49 (4) (2019 Jul) 302–312, <https://doi.org/10.1053/j.semnuclmed.2019.02.008>. Epub 2019 Apr 30. PMID: 31227053.
- [5] H. Wang, Y. Byun, C. Barinka, M. Pullambhatla, H.E. Bhang, J.J. Fox, J. Lubkowski, R.C. Mease, M.G. Pomper, Biososterism of urea-based GCPII inhibitors: synthesis and structure-activity relationship studies, *Bioorg. Med. Chem. Lett.* 20 (1) (2010 Jan 1) 392–397, <https://doi.org/10.1016/j.bmcl.2009.10.061>. Epub 2009 Oct 24. PMID: 19897367; PMCID: PMC2818328.
- [6] C. Barinka, Y. Byun, C.L. Dusich, S.R. Banerjee, Y. Chen, M. Castanares, A. P. Kozikowski, R.C. Mease, M.G. Pomper, J. Lubkowski, Interactions between human glutamate carboxypeptidase II and urea-based inhibitors: structural characterization, *J. Med. Chem.* 51 (24) (2008 Dec 25) 7737–7743, <https://doi.org/10.1021/jm800765e>. PMID: 19053759; PMCID: PMC5516903.
- [7] C. Barinka, Y. Byun, C.L. Dusich, S.R. Banerjee, Y. Chen, M. Castanares, A. P. Kozikowski, R.C. Mease, M.G. Pomper, J. Lubkowski, Interactions between human glutamate carboxypeptidase II and urea-based inhibitors: structural characterization, *J. Med. Chem.* 51 (24) (2008 Dec 25) 7737–7743, <https://doi.org/10.1021/jm800765e>. PMID: 19053759; PMCID: PMC5516903.
- [8] C. Barinka, M. Rinnová, P. Sácha, C. Rojas, P. Majer, B.S. Slusher, J. Konvalinka, Substrate specificity, inhibition and enzymological analysis of recombinant human glutamate carboxypeptidase II, *J. Neurochem.* 80 (3) (2002 Feb) 477–487, <https://doi.org/10.1046/j.0022-3042.2001.00715.x>. PMID: 11905994.
- [9] Jens Cardinale, Mareike Roscher, Martin Schäfer, Max Geerlings, Martina Benešová, Ulrike Bauder-Wüst, Yvonne Remde, Matthias Eder, Zora Nováková, Lucia Motlová, Cyril Barinka, Frederik L. Giesel, Klaus Kopka, Development of PSMA-1007-related series of 18F-labeled glu-ureido-type PSMA inhibitors, *J. Med. Chem.* 63 (19) (2020) 10897–10907, <https://doi.org/10.1021/acs.jmedchem.9b01479>.
- [10] C. Sachpekidis, A. Afshar-Oromieh, K. Kopka, et al., 18F-PSMA-1007 multiparametric, dynamic PET/CT in biochemical relapse and progression of prostate cancer, *Eur. J. Nucl. Med. Mol. Imag.* 47 (2020) 592–602, <https://doi.org/10.1007/s00259-019-04569-0>.
- [11] F.L. Giesel, B. Hadaschik, J. Cardinale, J. Radtke, M. Vinsensia, W. Lehnert, C. Kesch, Y. Tolstov, S. Singer, N. Grabe, S. Duensing, M. Schäfer, O.C. Neels, W. Mier, U. Haberkorn, K. Kopka, C. Kratochwil, F-18 labelled PSMA-1007: biodistribution, radiation dosimetry and histopathological validation of tumor lesions in prostate cancer patients, *Eur. J. Nucl. Med. Mol. Imag.* 44 (4) (2017 Apr) 678–688, <https://doi.org/10.1007/s00259-016-3573-4>. Epub 2016 Nov 26. PMID: 27889802; PMCID: PMC5323462.
- [12] K. Sprute, V. Kramer, S.A. Koerber, M. Meneses, R. Fernandez, C. Soza-Ried, M. Eiber, W.A. Weber, I. Rauscher, K. Rahbar, M. Schaefer, T. Watabe, M. Uemura, S. Naka, N. Nonomura, J. Hatazawa, C. Schwab, V. Schütz, M. Hohenfellner, T. Holland-Letz, J. Debus, C. Kratochwil, H. Amaral, P.L. Choyke, U. Haberkorn, C. Sandoval, F.L. Giesel, Diagnostic accuracy of 18F-PSMA-1007 PET/CT imaging for lymph node staging of prostate carcinoma in primary and biochemical recurrence, *J. Nucl. Med.* 62 (2) (2021 Feb) 208–213, <https://doi.org/10.2967/jnumed.120.246363>. Epub 2020 Aug 17. PMID: 32817141; PMCID: PMC8679593.
- [13] S. Awenat, A. Piccardo, P. Carvoeiras, G. Signore, L. Giovannella, J.O. Prior, G. Treglia, Diagnostic role of 18F-PSMA-1007 PET/CT in prostate cancer staging: a systematic review, *Diagnostics* 11 (2021) 552, <https://doi.org/10.3390/diagnostics11030552>.
- [14] J. Cardinale, M. Roscher, M. Schäfer, M. Geerlings, M. Benešová, U. Bauder-Wüst, Y. Remde, M. Eder, Z. Nováková, L. Motlová, C. Barinka, F.L. Giesel, K. Kopka, Development of PSMA-1007-related series of 18F-labeled glu-ureido-type PSMA inhibitors, *J. Med. Chem.* 63 (19) (2020 Oct 8) 10897–10907, <https://doi.org/10.1021/acs.jmedchem.9b01479>. Epub 2020 Sep 22. PMID: 32852205.
- [15] J. Calais, F. Ceci, M. Eiber, T.A. Hope, M.S. Hofman, C. Rischpler, T. Bach-Gansmo, C. Nanni, B. Savir-Baruch, D. Elashoff, T. Grogan, M. Dahlbom, R. Slavik, J. Gartmann, K. Nguyen, V. Lok, H. Jadvaj, A.U. Kishan, M.B. Rettig, R.E. Reiter, W.P. Fendler, J. Czernin, 18F-fluciclovine PET-CT and 68Ga-PSMA-11 PET-CT in patients with early biochemical recurrence after prostatectomy: a prospective, single-centre, single-arm, comparative imaging trial, *Lancet Oncol.* 20 (9) (2019 Sep) 1286–1294, [https://doi.org/10.1016/S1470-2045\(19\)30415-2](https://doi.org/10.1016/S1470-2045(19)30415-2). Epub 2019 Jul 30. Erratum in: *Lancet Oncol.* 2019 Nov;20(11):e613. Erratum in: *Lancet Oncol.* 2020 Jun;21(6):e304. PMID: 31375469; PMCID: PMC7469487.
- [16] Sarah Piron, Jeroen Verhoeven, Christian Vanhove, Filip De Vos, Recent advancements in 18F-labeled PSMA targeting PET radiopharmaceuticals, *Nucl. Med. Biol.* 106–107 (2022) 29–51, <https://doi.org/10.1016/j.nucmedbio.2021.12.005>. ISSN 0969-8051.
- [17] I. Vierasu, N. Trotta, S. Albinini, et al., Clinical experience with 18F-JK-PSMA-7 when using a digital PET/CT, *European J Hybrid Imaging* 6 (2022) 6, <https://doi.org/10.1186/s41824-022-00128-3>.
- [18] M. Hohberg, C. Kobe, P. Kröpf, et al., Biodistribution and radiation dosimetry of [18F]-JK-PSMA-7 as a novel prostate-specific membrane antigen-specific ligand for PET/CT imaging of prostate cancer, *EJNMMI Res.* 9 (2019) 66, <https://doi.org/10.1186/s13550-019-0540-7>.
- [19] F. Dietlein, M. Hohberg, C. Kobe, B.D. Zlatopolskiy, P. Kröpf, H. Endepols, P. Täger, J. Hammes, A. Heidenreich, B. Neumaier, A. Drzezga, M. Dietlein, An 18F-labeled PSMA ligand for PET/CT of prostate cancer: first-in-humans observational study and clinical experience with 18F-JK-PSMA-7 during the first year of application, *J. Nucl. Med.* 61 (2) (2020 Feb) 202–209, <https://doi.org/10.2967/jnumed.119.229542>. Epub 2019 Jul 19. PMID: 31324713.
- [20] F. Dietlein, P. Mueller, C. Kobe, H. Endepols, M. Hohberg, B.D. Zlatopolskiy, P. Kröpf, A. Heidenreich, B. Neumaier, A. Drzezga, M. Dietlein, [18F]-JK-PSMA-7 PET/CT under androgen deprivation therapy in advanced prostate cancer, *Mol. Imag. Biol.* 23 (2) (2021 Apr) 277–286, <https://doi.org/10.1007/s11307-020-01546-0>. Epub 2020 Oct 1. PMID: 33006028; PMCID: PMC7910246.
- [21] B.D. Zlatopolskiy, H. Endepols, P. Kröpf, M. Guliyev, E.A. Urusova, R. Richarz, M. Hohberg, M. Dietlein, A. Drzezga, B. Neumaier, Discovery of 18F-JK-PSMA-7, a PET probe for the detection of small PSMA-positive lesions, *J. Nucl. Med.* 60 (6) (2019 Jun) 817–823, <https://doi.org/10.2967/jnumed.118.218495>. Epub 2018 Nov 2. PMID: 30389823; PMCID: PMC6581226.
- [22] C.H. Yeong, M.H. Cheng, K.H. Ng, Therapeutic radionuclides in nuclear medicine: current and future prospects, *J. Zhejiang Univ. - Sci. B* 15 (10) (2014 Oct) 845–863, <https://doi.org/10.1631/jzus.B1400131>. PMID: 25294374; PMCID: PMC4201313.
- [23] A. Sanchez-Crespo, Comparison of Gallium-68 and Fluorine-18 imaging characteristics in positron emission tomography, *Appl. Radiat. Isot.* 76 (2013 Jun) 55–62, <https://doi.org/10.1016/j.apradiso.2012.06.034>. Epub 2012 Aug 29. PMID: 23063597.

- [24] F. Borgna, L.M. Deberle, S. Cohrs, R. Schibli, C. Müller, Combined application of albumin-binding [<sup>177</sup>Lu]Lu-PSMA-ALB-56 and fast-cleared PSMA inhibitors: optimization of the pharmacokinetics, *Mol. Pharm.* 17 (6) (2020 Jun 1) 2044–2053, <https://doi.org/10.1021/acs.molpharmaceut.0c00199>. Epub 2020 May 8. PMID: 32383887.
- [25] H.R. Kulkarni, A. Singh, C. Schuchardt, K. Niepsch, M. Sayeg, Y. Leshch, H. J. Wester, R.P. Baum, PSMA-based radioligand therapy for metastatic castration-resistant prostate cancer: the Bad Berka experience since 2013, *J. Nucl. Med.* 57 (Suppl 3) (2016 Oct) 97S–104S, <https://doi.org/10.2967/jnumed.115.170167>. PMID: 27694180.
- [26] K. Rahbar, H. Ahmadzadehfar, C. Kratochwil, U. Haberkorn, M. Schäfers, M. Essler, R.P. Baum, H.R. Kulkarni, M. Schmidt, A. Drzezga, P. Bartenstein, A. Pfestroff, M. Luster, U. Lützen, M. Marx, V. Prasad, W. Brenner, A. Heinzel, F.M. Mottaghy, J. Ruf, P.T. Meyer, M. Heuschkel, M. Eveslage, M. Bögemann, W.P. Fendler, B. J. Krause, German multicenter study investigating <sup>177</sup>Lu-PSMA-617 radioligand therapy in advanced prostate cancer patients, *J. Nucl. Med.* 58 (1) (2017 Jan) 85–90, <https://doi.org/10.2967/jnumed.116.183194>. Epub 2016 Oct 20. PMID: 27765862.
- [27] S. Debnath, N. Zhou, M. McLaughlin, S. Rice, A.K. Pillai, G. Hao, X. Sun, PSMA-targeting imaging and theranostic agents-Current status and future perspective, *Int. J. Mol. Sci.* 23 (2022) 1158.
- [28] L.B. Solnes, R.A. Werner, K.M. Jones, M.S. Sadaghiani, C.R. Bailey, C. Lapa, M. G. Pomper, S.P. Rowe, Theranostics: leveraging molecular imaging and therapy to impact patient management and secure the future of nuclear medicine, *J. Nucl. Med.* 61 (2020) 311–318.
- [29] R.A. Werner, X. Chen, C. Lapa, et al., The next era of renal radionuclide imaging: novel PET radiotracers, *Eur. J. Nucl. Med. Mol. Imag.* 46 (2019) 1773–1786, <https://doi.org/10.1007/s00259-019-04359-8>.
- [30] Novartis, Novartis receives European Commission approval for Pluvicto® as the first targeted radioligand therapy for treatment of progressive PSMA-positive metastatic castration-resistant prostate cancer. <https://www.novartis.com/news/media-releases/novartis-receives-european-commission-approval-pluvicto-first-targeted-radioligand-therapy-treatment-progressive-psma-positive-metastatic-castration-resistant-prostate-cancer>, 2022 accessed 14 April 2023.
- [31] Zhihao Zha, Seok Rye Choi, Linlin Li, Ruiyue Zhao, Karl Ploessl, Xinyue Yao, David Alexoff, Lin Zhu, Hank F. Kung, *J. Med. Chem.* 65 (19) (2022) 13001–13012, <https://doi.org/10.1021/acs.jmedchem.2c00852>.
- [32] C.A. D'Souza, W.J. McBride, R.M. Sharkey, L.J. Todaro, D.M. Goldenberg, High-yielding aqueous 18F-labeling of peptides via Al18F chelation, *Bioconjugate Chem.* 22 (9) (2011 Sep 21) 1793–1803, <https://doi.org/10.1021/bc200175c>. Epub 2011 Aug 9. PMID: 21805975; PMCID: PMC3178738.
- [33] M. Meisenheimer, Y. Saenko, E. Eppard, Gallium-68: radiolabeling of radiopharmaceuticals for PET imaging - a lot to consider. *Medical isotopes*, Intech (2021), <https://doi.org/10.5772/intechopen.90615>.
- [34] Drishty Satpati, *Bioconjugate Chem.* 32 (3) (2021) 430–447, <https://doi.org/10.1021/acs.bioconjchem.1c00010>.
- [35] J. Kleynhans, S. Rubow, J. le Roux, B. Marjanovic-Painter, J.R. Zeevaert, T. Ebenhan, Production of [68Ga]Ga-PSMA: comparing a manual kit-based method with a module-based automated synthesis approach, *J. Label. Compd. Radiopharm.* 63 (2020) 553–563, <https://doi.org/10.1002/jlcr.3879>.
- [36] W.J. McBride, R.M. Sharkey, H. Karacay, C.A. D'Souza, E.A. Rossi, P. Laverman, C. H. Chang, O.C. Boerman, D.M. Goldenberg, A novel method of 18F radiolabeling for PET, *J. Nucl. Med.* 50 (6) (2009 Jun) 991–998, <https://doi.org/10.2967/jnumed.108.060418>. Epub 2009 May 14. PMID: 19443594.
- [37] William J. McBride, Christopher A. D'Souza, Robert M. Sharkey, Habibe Karacay, Edmund A. Rossi, Chien-Hsing Chang, and David M. Goldenberg, *Bioconjugate Chem.* 21 (7) (2010) 1331–1340, <https://doi.org/10.1021/bc100137x>.
- [38] S. Lütje, G.M. Franssen, K. Herrmann, O.C. Boerman, M. Rijpkema, M. Gotthardt, In vitro and in vivo characterization of an 18 F-AlF<sub>3</sub>-labeled PSMA ligand for imaging of PSMA-expressing xenografts, *J Nucl Med. Society of Nuclear Medicine Inc.* (2019) 1017–1022. <http://jnm.snmjournals.org/lookup/doi/10.2967/jnumed.118.218941>.
- [39] S. Boschi, J.T. Lee, S. Beykan, R. Slavik, L. Wei, C. Spick, U. Eberlein, A.K. Buck, F. Lodi, G. Cicoria, J. Czernin, M. Lassmann, S. Fanti, K. Herrmann, Synthesis and preclinical evaluation of an Al18F radiofluorinated GLU-UREA-LYS(AHX)-HBED-CC PSMA ligand, *Eur. J. Nucl. Med. Mol. Imag.* 43 (12) (2016 Nov) 2122–2130, <https://doi.org/10.1007/s00259-016-3437-y>. Epub 2016 Jun 22. PMID: 27329046; PMCID: PMC5050145.
- [40] S. Piron, J. Verhoeven, B. Descamps, et al., Intra-individual dynamic comparison of 18F-PSMA-11 and 68Ga-PSMA-11 in LNCaP xenograft bearing mice, *Sci. Rep.* 10 (2020), 21068, <https://doi.org/10.1038/s41598-020-78273-7>.
- [41] S. Piron, K. De Man, N. Van Laeken, Y. D'Asseler, K. Bacher, K. Kersemans, P. Ost, K. Decaestecker, P. Deseyne, V. Fonteyne, N. Lumen, E. Achten, B. Brans, F. De Vos, Radiation dosimetry and biodistribution of 18F-PSMA-11 for PET imaging of prostate cancer, *J. Nucl. Med.* 60 (12) (2019 Dec) 1736–1742, <https://doi.org/10.2967/jnumed.118.225250>. Epub 2019 Apr 26. PMID: 31028165.
- [42] Gerardo dos Santos, Monica Rodriguez Taroco, Javier Giglio, Eduardo Savio, Omar Alonso *Journal of Nuclear Medicine* 61 (supplement 1) (May 2020) 1268.
- [43] E. Al-Momani, I. Israel, S. Samnick, Validation of a [Al18F]PSMA-11 preparation for clinical applications, *Appl. Radiat. Isot.* 130 (2017 Dec) 102–108, <https://doi.org/10.1016/j.apradiso.2017.09.003>. Epub 2017 Sep 6. PMID: 28950199.
- [44] Joseph A. Ioppolo, Rikki A. Nezhich, Kirsty L. Richardson, Laurence Morandau, Peter J. Leadman, Roger I. Price, Direct in vivo comparison of [18F]PSMA-1007 with [68Ga]Ga-PSMA-11 and [18F]AlF<sub>3</sub>-PSMA-11 in mice bearing PSMA-expressing xenografts, *Appl. Radiat. Isot.* 161 (2020), 109164, <https://doi.org/10.1016/j.apradiso.2020.109164>. ISSN 0969-8043.
- [45] X. Zhou, X. Jiang, L. Liu, X. Wang, C. Li, Y. Yao, Y. Kou, J. Shen, T. Shen, Z. Li, S. Yang, S. Zhou, H. Liao, Z. Luo, X. Wu, S. Chen, Z. Cheng, Evaluation of 18F-PSMA-1007 PET/CT in prostate cancer patients with biochemical recurrence after radical prostatectomy, *Transl Oncol* 15 (1) (2022 Jan), 101292, <https://doi.org/10.1016/j.tranon.2021.101292>. Epub 2021 Nov 24. PMID: 34837847; PMCID: PMC8633368.
- [46] J.J. Morigi, P.D. Stricker, P.J. van Leeuwen, R. Tang, B. Ho, Q. Nguyen, G. Hruby, G. Fogarty, R. Jagavkar, A. Kneebone, A. Hickey, S. Fanti, L. Tarlinton, L. Emmett, Prospective comparison of 18F-fluoromethylcholine versus 68Ga-PSMA PET/CT in prostate cancer patients who have rising PSA after curative treatment and are being considered for targeted therapy, *J. Nucl. Med.* 56 (8) (2015 Aug) 1185–1190, <https://doi.org/10.2967/jnumed.115.160382>. Epub 2015 Jun 25. PMID: 26112024.
- [47] J. Calais, W.P. Fendler, K. Herrmann, M. Eiber, F. Ceci, Comparison of 68Ga-PSMA-11 and 18F-fluciclovine PET/CT in a case series of 10 patients with prostate cancer recurrence, *J. Nucl. Med.* 59 (5) (2018 May) 789–794, <https://doi.org/10.2967/jnumed.117.203257>. Epub 2017 Dec 14. PMID: 29242404.
- [48] K. Sprute, V. Kramer, S.A. Koerber, M. Meneses, R. Fernandez, C. Soza-Ried, M. Eiber, W.A. Weber, I. Rauscher, K. Rahbar, M. Schaefer, T. Watabe, M. Uemura, S. Naka, N. Nonomura, J. Hatazawa, C. Schwab, V. Schütz, M. Hohenfellner, T. Holland-Letz, J. Debus, C. Kratochwil, H. Amaral, P.L. Choyke, U. Haberkorn, C. Sandoval, F.L. Giesel, Diagnostic accuracy of 18F-PSMA-1007 PET/CT imaging for lymph node staging of prostate carcinoma in primary and biochemical recurrence, *J. Nucl. Med.* 62 (2) (2021 Feb) 208–213, <https://doi.org/10.2967/jnumed.120.246363>. Epub 2020 Aug 17. PMID: 32817141; PMCID: PMC8679593.
- [49] J.A. Ioppolo, R.A. Nezhich, K.L. Richardson, L. Morandau, P.J. Leadman, R.I. Price, Direct in vivo comparison of [18F]PSMA-1007 with [68Ga]Ga-PSMA-11 and [18F]AlF<sub>3</sub>-PSMA-11 in mice bearing PSMA-expressing xenografts, *Appl. Radiat. Isot.* 161 (2020 Jul), 109164, <https://doi.org/10.1016/j.apradiso.2020.109164>. Epub 2020 Apr 2. PMID: 32321698.
- [50] J. Kuten, I. Fahoum, Z. Savin, O. Shamni, G. Gitstein, D. Hershkovitz, N. J. Mobjeesh, O. Yossepovitch, E. Mishani, E. Even-Sapir, Head-to-Head comparison of 68Ga-PSMA-11 with 18F-PSMA-1007 PET/CT in staging prostate cancer using histopathology and immunohistochemical analysis as a reference standard, *J. Nucl. Med.* 61 (4) (2020 Apr) 527–532, <https://doi.org/10.2967/jnumed.119.234187>. Epub 2019 Sep 27. PMID: 31562225.
- [51] N. Fennessy, J. Lee, J. Shin, B. Ho, S.A. Ali, R. Paschkewitz, L. Emmett, Frusemide aids diagnostic interpretation of 68 Ga-PSMA positron emission tomography/CT in men with prostate cancer, *J Med Imaging Radiat Oncol* 61 (6) (2017 Dec) 739–744, <https://doi.org/10.1111/1754-9485.12625>. Epub 2017 Jun 17. PMID: 28623852.
- [52] T. Ganguly, S. Danno, M.R. Hopkins, S. Murphy, H. Cahaya, J.E. Blecha, S. Jivan, C.R. Drake, C. Barinka, E.F. Jones, H.F. VanBroeklin, C.E. Berkman, A high-affinity [(18)F]-labeled phosphoramidate peptidomimetic PSMA-targeted inhibitor for PET imaging of prostate cancer, *Nucl. Med. Biol.* 42 (10) (2015 Oct) 780–787, <https://doi.org/10.1016/j.nucmedbio.2015.06.003>. Epub 2015 Jun 9. PMID: 26169882; PMCID: PMC4624265.
- [53] Y. Huang, H. Li, S. Ye, G. Tang, Y. Liang, K. Hu, Synthesis and preclinical evaluation of an Al18F radiofluorinated bivalent PSMA ligand, *Eur. J. Med. Chem.* 221 (2021 Oct 5), 113502, <https://doi.org/10.1016/j.ejmech.2021.113502>. Epub 2021 May 1. PMID: 33965863.
- [54] S. Robu, A. Schmidt, M. Eiber, et al., Synthesis and preclinical evaluation of novel 18F-labeled Glu-urea-Glu-based PSMA inhibitors for prostate cancer imaging: a comparison with 18F-DCFPyl and 18F-PSMA-1007, *EJNMMI Res.* 8 (2018) 30, <https://doi.org/10.1186/s13550-018-0382-8>.
- [55] M.S. Dennis, M. Zhang, Y.G. Meng, M. Kadkhodayan, D. Kirchofer, D. Combs, L. A. Damico, Albumin binding as a general strategy for improving the pharmacokinetics of proteins, *J. Biol. Chem.* 277 (38) (2002 Sep 20) 35035–35043, <https://doi.org/10.1074/jbc.M205854200>. Epub 2002 Jul 15. PMID: 12119302.
- [56] A. Constantinou, C. Chen, M.P. Deonaran, Modulating the pharmacokinetics of therapeutic antibodies, *Biotechnol. Lett.* 32 (5) (2010 May) 609–622, <https://doi.org/10.1007/s10529-010-0214-z>. Epub 2010 Feb 4. PMID: 20131077.
- [57] C. Kesch, M. Vinsensia, J.P. Radtke, H.P. Schlemmer, M. Heller, E. Ellert, T. Holland-Letz, S. Duensing, N. Grabe, A. Afshar-Oromieh, K. Wiecezrek, M. Schäfer, O.C. Neels, J. Cardinale, C. Kratochwil, M. Hohenfellner, K. Kopka, U. Haberkorn, B.A. Hadaschik, F.L. Giesel, Intra-individual comparison of 18F-PSMA-1007 PET/CT, multiparametric MRI, and radical prostatectomy specimens in patients with primary prostate cancer: a retrospective, proof-of-concept study, *J. Nucl. Med.* 58 (11) (2017 Nov) 1805–1810, <https://doi.org/10.2967/jnumed.116.189233>. Epub 2017 May 4. Erratum in: *J Nucl Med.* 2019 Apr;60(4): 554. PMID: 28473595.
- [58] B.M. Privé, B. Israël, M.G.M. Schilham, et al., Evaluating F-18-PSMA-1007-PET in primary prostate cancer and comparing it to multi-parametric MRI and histopathology, *Prostate Cancer Prostatic Dis.* 24 (2021) 423–430, <https://doi.org/10.1038/s41391-020-00292-2>.
- [59] H. Xu, H. Wang, Z. Xu, S. Bian, Z. Xu, H. Zhang, The multifaceted roles of peptides in "always-on" near-infrared fluorescent probes for tumor imaging, *Bioorg. Chem.* 129 (2022 Dec), 106182, <https://doi.org/10.1016/j.bioorg.2022.106182>. Epub 2022 Oct 19. PMID: 36341739.
- [60] A. Mollica, A. Carotenuto, E. Novellino, A. Limatola, R. Costante, F. Pinnen, A. Stefanucci, S. Pieretti, A. Borsodi, R. Samavati, F. Zador, S. Benyhe, P. Davis, F. Porreca, V.J. Hruby, Novel cyclic biphalin analogue with improved antinociceptive properties, *ACS Med. Chem. Lett.* 5 (9) (2014 Jul 14) 1032–1036, <https://doi.org/10.1021/ml500241n>. PMID: 25221662; PMCID: PMC4160744.
- [61] A. Mollica, F. Pinnen, F. Feliciani, A. Stefanucci, G. Lucente, P. Davis, F. Porreca, S. W. Ma, J. Lai, V.J. Hruby, New potent biphalin analogues containing p-fluoro-L-phenylalanine at the 4,4' positions and non-hydrazone linkers, *Amino Acids* 40 (5)

- (2011 May) 1503–1511, <https://doi.org/10.1007/s00726-010-0760-7>. Epub 2010 Oct 6. PMID: 20924622; PMCID: PMC5689474.
- [62] A. Mollica, R. Costante, A. Stefanucci, F. Pinnen, G. Lucente, S. Fidanza, S. Pieretti, Antinociceptive profile of potent opioid peptide AM94, a fluorinated analogue of biphalin with non-hydrazine linker, *J. Pept. Sci.* 19 (4) (2013 Apr) 233–239, <https://doi.org/10.1002/psc.2465>. Epub 2012 Nov 8. PMID: 23136069.
- [63] A. Stefanucci, W. Lei, V.J. Hruby, G. Macedonio, G. Luisi, S. Carradori, J. M. Streicher, A. Mollica, Fluorescent-labeled bioconjugates of the opioid peptides biphalin and DPDPE incorporating fluorescein-maleimide linkers, *Future Med. Chem.* 9 (9) (2017 Jun) 859–869, <https://doi.org/10.4155/fmc-2016-0232>. Epub 2017 Jun 21. PMID: 28635314.
- [64] A. Stefanucci, M.P. Dimmito, G. Molnar, J.M. Streicher, E. Novellino, G. Zengin, A. Mollica, Developing cyclic opioid analogues: fluorescently labeled bioconjugates of biphalin, *ACS Med. Chem. Lett.* 11 (5) (2020 Jan 8) 720–726, <https://doi.org/10.1021/acsmchemlett.9b00569>. PMID: 32435376; PMCID: PMC7236251.
- [65] J. Lau, E. Rousseau, D. Kwon, K.-S. Lin, F. Bénard, X. Chen, Insight into the development of PET radiopharmaceuticals for oncology, *Cancers* 12 (2020) 1312, <https://doi.org/10.3390/cancers12051312>.
- [66] S.W. Oh, G.J. Cheon, Prostate-specific membrane antigen PET imaging in prostate cancer: opportunities and challenges, *Korean J. Radiol.* 19 (5) (2018 Sep-Oct) 819–831, <https://doi.org/10.3348/kjr.2018.19.5.819>. Epub 2018 Aug 6. PMID: 30174470; PMCID: PMC6082771.